PRAMANA — journal of physics

Vol. 66, No. 4
April 2006
pp. 709–729

Hadrons in medium

U MOSEL
Institut fuer Theoretische Physik, Universitaet Giessen, D-35392 Giessen, Germany
E-mail: Ulrich.Mosel@theo.physik.uni-giessen.de

Abstract. In these lectures I first give the motivation for investigations of in-medium properties of hadrons. I discuss the relevant symmetries of QCD and how they might affect the observed hadron properties. I then discuss at length the observable consequences of in-medium changes of hadronic properties in reactions with elementary probes, and in particular photons, on nuclei. Here I put an emphasis on new experiments on changes of the σ- and ω-mesons in medium.

Keywords. Hadrons; QCD; nuclear medium.

PACS Nos 25.20.-x; 25.80.Ek; 24.85.+p; 13.60.Le

1. Introduction

Studies of in-medium properties of hadrons are driven by a number of – partly connected – motivations. The first motivation for the study of hadronic in-medium properties is provided by our interest in understanding the structure of large dense systems, such as the interior of stars. This structure obviously depends on the composition of stellar matter and its interactions (for a recent review, see [1]).

The second motivation is based on the expectation that changes of hadronic properties in medium can be precursor phenomena to changes in the phase structure of nuclear matter. Here the transition to the chirally symmetric phase, that exhibits manifestly the symmetries of the underlying theory of strong interactions, i.e. QCD, is of particular interest. Present day's ultrarelativistic heavy-ion collisions explore this phase boundary in the limit of high temperatures ($T \approx 170$ MeV) and low densities. The other limit (low temperatures and high densities) is harder to reach, although the older AGS heavy-ion experiments and the planned CBM experiment at the new FAIR facility [2] may yield insight into this area. However, even in these experiments the temperatures reached are still sizeable ($T \approx 120$ MeV). At very low temperatures the only feasible method seems to be the exploration of the hadronic structure inside ordinary nuclei, at the prize of a low density. Here the temperature is $T = 0$ and the density at most equals the equilibrium density of nuclear matter, ρ_0. It is thus of great interest to explore if such low densities can already give precursor signals for chiral symmetry restoration.

That hadrons can indeed change their properties and couplings in the nuclear medium has been well-known to nuclear physicists since the days of the delta-hole model that dealt with the changes of the properties of the pion and delta-resonance inside nuclei [3]. Due to the predominant p-wave interaction of pions with nucleons one observes here a lowering of the pion branch with increasing pion momentum and nucleon density. This effect can be seen in optical model analyses of pion scattering on nuclei, but the absorptive part of the π-nucleus interaction limits the sensitivity to small densities. More recently, experiments at the FSR at GSI have also shown that the mass of a pion at rest in the nuclear medium differs from its value in vacuum [4]. This is interesting since there are also recent experiments [5] that look for in-medium changes of the σ-meson, the chiral partner of the pion. Any comparison of scalar and pseudoscalar strength could thus give information about the degree of chiral symmetry restoration in nuclear matter.

In addition, experiments for charged kaon production at GSI [6] have given some evidence for the theoretically predicted lowering of the K^- mass in medium and the (weaker) rising of the K^+ mass. State-of-the-art calculations of the in-medium properties of kaons have shown that the usual quasi-particle approximation for these particles is no longer justified inside nuclear matter where they acquire a broad spectral function [7,8].

At higher energies, at the CERN SPS and most recently at the Brookhaven RHIC, in-medium changes of vector mesons have found increased interest. This was due to two main reasons. First, these mesons are the first excitations of the QCD vacuum that are not protected by chiral symmetry, as the pions as Goldstone bosons are, and should therefore be more directly related to the chiral condensates. This expectation was triggered by the original work of Hatsuda and Lee [9] that, based on QCD sum rules, predicted a significant lowering of the vector meson masses with increasing density, the effect being as large as 30% already at nuclear matter equilibrium density. As discussed in [10,11] this original prediction strongly depended on simplifying assumptions for the spectral function of the particles involved. When more realistic spectral shapes are used, the QCD sum rule gives only certain restrictions on mass and width of the particles involved, but does not fix the latter; hadronic models are needed for that. In particular, for the ρ-meson it turned out that the broadening is more dominant than a mass-shift [12].

The second reason for the interest in vector meson production stems from the fact that these mesons couple strongly to the photon so that electromagnetic signals can yield information about properties of hadrons deeply embedded in the nuclear matter. Indeed, the CERES experiment [13] has found a considerable excess of dileptons in an invariant mass range from $\approx$300 MeV to $\approx$700 MeV as compared to the expectations based on the assumption of freely radiating mesons.

This result has found an explanation in terms of a shift of the ρ-meson spectral function down to lower masses, as expected from theory (see, e.g., [12,14–16]). However, the actual reason for the observed dilepton excess is far from clear. Both models that just shift the pole mass of the vector meson as well as those that also modify the spectral shape have successfully explained the data [17–19]; in addition, even a calculation that just used the free radiation rates with their – often quite large – experimental uncertainties was compatible with the observations [20]. There are also calculations that attribute the observed effect to radiation from a quark–gluon plasma [21].

The more recent experimental results on a change of the ρ-meson properties in-medium obtained in an ultrarelativistic Au + Au collision by the STAR Collaboration at RHIC [22] show a downward shift of the ρ-meson pole mass by about 70 MeV. Since the $p + p$ data obtained in the same experiment also show a similar, though slightly less pronounced (-40 MeV), shift of the ρ-meson mass, phase-space distortions of the ρ-meson spectral shape may be at least partly responsible for the observed mass-shift. In the heavy-ion experiment then a number of additional effects, mainly by dynamical interactions with surrounding matter, may contribute, but are hard to separate from the more mundane phase-space effects [23].

For both experiments quite different model calculations tend to explain the data, though often with some model assumptions. Their theoretical input is sufficiently different as to make the inverse conclusion that the data prove one or another of the proposed explanations impossible. In particular, if one is after some 'exotic' effect like a signal for the QGP, one has to make sure that one understands the 'classical' contributions to the observed signals very well.

I have therefore proposed to look for the theoretically predicted changes of vector meson properties inside the nuclear medium in reactions on normal nuclei with more microscopic probes [24,25]. Of course, the nuclear density felt by the vector mesons in such experiments lies much below the equilibrium density of nuclear matter, ρ_0, so that naively any density-dependent effects are expected to be much smaller than in heavy-ion reactions.

On the other hand, there is a big advantage to these experiments: they proceed with the spectator matter being close to its equilibrium state. This is essential because all theoretical predictions of in-medium properties of hadrons are based on an equilibrium model in which the hadron (vector meson) under investigation is embedded in cold nuclear matter in equilibrium and with infinite extension. However, a relativistic heavy-ion reaction proceeds – at least initially – far from equilibrium. Even if equilibrium is reached in a heavy-ion collision this state changes by cooling through expansion and particle emission and any observed signal is built up by integrating over the emissions from all these different stages of the reaction.

Calculations of in-medium properties of hadrons thus necessarily rely on a number of simplifying assumptions, foremost being that of an infinite medium at rest in which the hadron under study is embedded. The properties so calculated are then, in a second step, being locally inserted into a time-dependent event simulation. In actual experiments these hadrons are observed through their decay products and these have to travel through the surrounding nuclear matter to the detectors. Except for the case of electromagnetic signals (photons, dileptons) this is connected with often sizeable final state interactions (FSI) that have to be treated as realistic as possible. For a long time, the Glauber approximation which allows only for absorptive processes along a straight-line path has been the method of choice in theories of photonuclear reactions on nuclei. This may be sufficient if one is only interested in total yields of strongly absorbed particles. However, it is clearly insufficient when one aims at, for example, reconstructing the spectral function of a hadron inside the matter through its decay products. Rescattering and sidefeeding through coupled channel effects can affect the final result so that a realistic description of such effects is absolutely mandatory [26].

In this lecture note I first outline the fundamentals of chiral symmetry, its expected density dependence and its connection with actual observables. I then summarize results that we have obtained in studies of observable consequences of in-medium changes of hadronic spectral functions in reactions of elementary probes with nuclei. I demonstrate that the expected in-medium sensitivity in such reactions is as high as that in relativistic heavy-ion collisions and that in particular photonuclear reactions present an independent, cleaner testing ground for assumptions made in analyzing heavy-ion reactions.

2. Theory

2.1 *Chiral symmetry*

A large part of the current interest in in-medium properties of hadrons comes from the hope to learn something about quarks in nuclei. More specifically, one hopes to see precursors of a restoration of the original symmetries of the theory of strong interactions, i.e. QCD, which are spontaneously broken in our world. In this section of the lecture, I briefly summarize the – for the present discussion – most relevant features of QCD. The material here draws heavily on my book [27] where many more details can be found.

The QCD Lagrangian

$$\mathcal{L}_{\mathrm{QCD}} = -\frac{1}{4} G^c_{\mu\nu} G^{c\mu\nu} + \sum_f \left[\bar{q}_f (\mathrm{i}\gamma^\mu D_\mu - m_f) q_f\right] \tag{1}$$

describes all the strong interactions of color-triplets q representing the quarks. Here the sum over c runs over the eight members of the color octet and D_μ is given by

$$D_\mu = \partial_\mu + \mathrm{i}g \frac{\lambda^c}{2} G^c_\mu. \tag{2}$$

The G^c_μ represents the eight vector fields describing the gauge bosons of the theory, called 'gluons', because they transmit the binding forces and $G_{\mu\nu}$ in (1) denotes the corresponding field tensor. g is a dimensionless coupling constant (for further details, see Chap. 15 in [27]).

If one assumes that the masses of the up- and down-quarks are nearly the same, then QCD possesses a global $SU(2)_V$ symmetry under the transformation

$$q_c(x) \rightarrow q'_c(x) = \sum_{f=1}^{3} \mathrm{e}^{-\mathrm{i}\varepsilon^f (\lambda^f/2)} q_c(x) \tag{3}$$

which acts onto the flavor degrees of freedom of the quark spinor given by

$$q_c(x) = \begin{pmatrix} u_c(x) \\ d_c(x) \\ s_c(x) \end{pmatrix}, \tag{4}$$

where u_c, d_c and s_c represent the up, down and strange quark, respectively, with a color index c. The sum over the flavor index f in eq. (3) runs only from 1 to 3, i.e. over the generators λ^f of the $SU(2)$ subgroup of the full flavor-$SU(3)$. As a consequence of the invariance of $\mathcal{L}_{\rm QCD}$ under the transformation (3), the flavor vector current

$$V_\mu^f(x) = \bar{q}_c \gamma_\mu \frac{\lambda^f}{2} q_c \quad (f = 1, 2, 3) \tag{5}$$

is conserved on the quark level. The observed isospin symmetry of strong interactions and the corresponding vector current conservation (CVC) can thus be understood as a consequence of a symmetry of quark–quark interactions.

If, in addition, $m_u = m_d = 0$, then there is also a symmetry of the QCD Lagrangian under

$$q_c(x) \to q_c'(x) = \sum_{f=1}^{3} \mathrm{e}^{-\mathrm{i}\gamma_5 \varepsilon^f (\lambda^f/2)} q_c(x), \tag{6}$$

so that the axial vector current

$$A_\mu^f = \bar{q}_c \gamma_\mu \gamma_5 \frac{\lambda^f}{2} q_c \quad (f = 1, 2, 3) \tag{7}$$

is also conserved. In these considerations one uses the fact that the gluon fields G_μ^c are pure color fields and are thus not affected by the flavor generators λ^f or by the Dirac algebra, e.g. by γ_5.

It is clear that the chiral symmetry cannot be a manifest one on the hadronic level, since the hadrons are all massive. However, the Goldstone mechanism of spontaneous symmetry breaking can reconcile the non-zero masses of the hadrons with the observed (partial) conservation of the axial current. The axial $SU(2)$ symmetry is then assumed to be realized in the Goldstone mode in which the Lagrangian, but not the state of the system, possesses the axial $SU(2)$ symmetry. Therefore, it is obvious that in the real world also the chiral symmetry must be spontaneously broken. An order parameter for this symmetry breaking is given by the so-called chiral condensate

$$\langle |\bar{q}q| \rangle \neq 0, \tag{8}$$

where the expectation value is taken in the vacuum state. The chiral condensate and thus the ground state can be chirally symmetric only if this condensate is zero as one can show by applying the transformation (6) (see also discussion below).

A very simple estimate shows that the chiral condensate in the nuclear medium is in lowest order in density given by [16]

$$\langle \bar{q}q \rangle_{\rm med}(\rho, T) \approx \left(1 - \sum_h \frac{\Sigma_h \rho_h^s(\rho, T)}{f_\pi^2 m_\pi^2} \right) \langle \bar{q}q \rangle_{\rm vac}. \tag{9}$$

Here $\rho_{\rm s}$ is the *scalar* density of the hadron h in the nuclear system and Σ_h the so-called sigma-commutator that contains information on the chiral properties of

h. The sum runs over all hadronic states. While (9) is nearly exact, its actual value is limited because neither the sigma-commutators of the higher lying hadrons nor their scalar densities are known. However, at very low temperatures close to the ground state these are accessible for the nucleon. Here $\rho_{\rm s} \approx \rho_{\rm v}(m/E)$ so that the condensate drops linearly with the nuclear (vector) density. Inserting numerical values for the physical constants in (9) gives

$$\langle \bar{q}q \rangle_{\rm med}(\rho, 0) \approx \left(1 - 0.3\frac{\rho}{\rho_0}\right) \langle \bar{q}q \rangle_{\rm vac}. \tag{10}$$

This drop of the chiral condensate with density can be understood in physical terms: with increasing density the hadrons with their chirally symmetric phase in their interior fill in more and more space in the vacuum with its spontaneously broken chiral symmetry. Note that this is a pure volume effect; it is there already for a free, non-interacting hadron gas. One can obtain a very simple estimate for this effect by assuming that inside the baryons the chirally symmetric phase prevails, as it does in bag models, (for a review of such models see [27]). Assuming a baryon radius of ≈0.8 fm one obtains $V_N \approx 2.1$ fm^3. This number has to be compared with the specific volume of one baryon at normal nuclear matter density ($\rho_0 = 0.15\,{\rm fm}^{-3}$): $v = 0.15^{-1}\,{\rm fm}^3 \approx 6.7\,{\rm fm}^3$. This shows that at about $v/V_N \approx 3$ times nuclear equilibrium density the baryons significantly overlap so that their chirally restored phase fills all space.

Often, the so-called Nambu–Jona–Lasinio (NJL) model has also been used to determine the drop of the chiral condensate with density (and temperature) and to establish a link between the chiral condensate and physical masses. In this model, the QCD Lagrangian is replaced by a Lagrangian that exhibits the chiral symmetry of QCD manifestly and in which the gluon fields are assumed to be integrated out. The interactions mediated by them are modeled by a point-interaction of the quarks. The NJL model in the two-flavor version is given by

$$\mathcal{L} = {\rm i}\bar{q}\gamma_\mu\partial^\mu q + G[(\bar{q}q)^2 + (\bar{q}{\rm i}\gamma_5\vec{\tau}q)^2]. \tag{11}$$

While the authors originally formulated this model in terms of nucleon fields (quarks were not known then) we have given here the Lagrangian in terms of quark fields q. The Lagrangian (11) represents a system of massless fermions interacting through a contact interaction (the term in square brackets). The constant G is a coupling constant with the dimension of (mass)$^{-2}$; it is assumed to be positive so that the self-interaction of the quark fields is attractive. Since the interaction is local it corresponds to a δ-function two-body potential between the quarks in a non-relativistic language.

In Hartree–Fock mean field theory the single particle Hamiltonian can be obtained by a variation of the vacuum energy corresponding to the NJL Lagrangian with respect to $\bar{q}$. The ensuing single-particle Hamiltonian exhibits a mass term

$$Mq = \frac{\delta\langle\mathcal{H}\rangle}{\delta\bar{q}} = -2G\langle\bar{q}q\rangle q. \tag{12}$$

The mass can be evaluated in a vacuum of free states

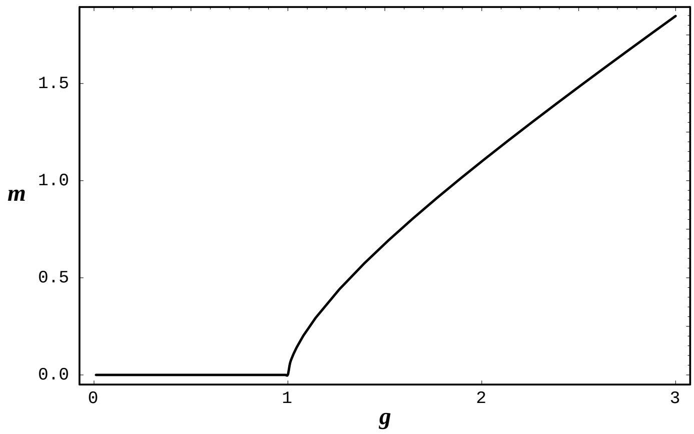

Figure 1. Scaled quark mass $m = M/\Lambda$ in the NJL model as a function of the scaled coupling constant $g = \Lambda^2/\pi^2 G$ for vanishing Fermi momentum (from [27]).

$$M = -2G\langle 0|\bar{q}q|0\rangle = 2G\frac{1}{V}\sum_{ps}\frac{M}{\sqrt{\vec{p}^2+M^2}}. \tag{13}$$

The sum over states in the Dirac sea diverges; it thus has to be regularized by introducing an appropriate cut-off Λ for the sum over momenta. Going over to an integral representation gives

$$M = 4G\int_{|\vec{p}|<\Lambda}\frac{M}{\sqrt{\vec{p}^2+M^2}}\frac{\mathrm{d}^3p}{(2\pi)^3}. \tag{14}$$

It is obvious that (14) has $M = 0$ as a solution, corresponding to a chirally symmetric vacuum (ground-) state. However, for large enough couplings also a solution with $M > 0$ is possible. In this case the vacuum state no longer exhibits the chiral symmetry of the underlying theory, QCD; the symmetry is spontaneously broken. The value of the 'chiral condensate' (12)

$$\langle\bar{q}q\rangle = -\frac{1}{V}\sum_{ps}\frac{M}{\sqrt{\vec{p}^2+M^2}} \tag{15}$$

gives a measure for the amount of chiral symmetry breaking: it is zero if chiral symmetry is present in the vacuum and non-zero otherwise. Equation (14) has exactly the same structure as the gap equation in the BCS theory of superconductivity, used, for example, to obtain the pairing gap as a function of the pairing interaction strength. The mass M plays here the role of the pairing gap Δ. The dependence of mass on coupling constant is shown in figure 1.

It is a well-known property of the gap equation that the gap decreases – and ultimately disappears – due to the blocking effect when states above the Fermi level become occupied, either through a thermal excitation of the system or through the presence of odd nucleons. Exactly the same phenomenon appears here: if positive energy quark states also are occupied, either through a temperature in the system or through a non-vanishing baryon density, the integral on the RHS of (14) extends over these states as well; because of the properties of the positive-energy spinors these states appear with an opposite sign and give a contribution to the mass

$$\Delta M = -4G \int_{|\vec{p}|<p_{\mathrm{F}}} \frac{M}{\sqrt{\vec{p}^2+M^2}} \frac{\mathrm{d}^3p}{(2\pi)^3}. \tag{16}$$

In order to compensate for this negative contribution, with G fixed, the masses then have to become smaller until they have to vanish altogether, when the occupation of the positive energy states is increased more and more. Thus, with increasing density the quarks become massless again and chiral symmetry is restored. The same effect takes place when the temperature of the system is increased. In that case states above the Fermi momentum are partially occupied and this blocking leads to a decrease of the mass, just as in BCS theory.

2.2 *QCD sum rules and hadronic models*

In the NJL model the dropping of the chiral condensate with density and/or temperature directly causes a drop of the mass because both are linearly proportional. This is no longer the case in complex hadronic systems. How the drop of the scalar condensate there translates into observable hadron masses is not uniquely prescribed. The only rigorous connection is given by the QCD sum rules that relates an integral over the hadronic spectral function to a sum over combination of quark and gluon condensates with powers of $1/Q^2$. The starting point for this connection is the electromagnetic current–current correlator

$$\Pi_{\mu\nu}(q) = i \int \mathrm{d}^4x\, \mathrm{e}^{iqx} \langle T j_\mu(x) j_\nu(0) \rangle\,, \tag{17}$$

where the current is expressed in terms of quark-field operators. This correlator can be decomposed [10] as

$$\Pi_{\mu\nu}(q) = q_\mu q_\nu R(q^2) - g_{\mu\nu} \Pi^{\mathrm{isotr}}(q^2)\,. \tag{18}$$

The QCD sum rule then reads

$$R^{\mathrm{OPE}}(Q^2) = \frac{\tilde{c}_1}{Q^2} + \tilde{c}_2 - \frac{Q^2}{\pi} \int_0^\infty \mathrm{d}s\, \frac{\mathrm{Im} R^{\mathrm{HAD}}(s)}{(s+Q^2)s} \tag{19}$$

with $Q^2 := -q^2 \gg 0$ and some subtraction constants $\tilde{c}_i$. Here R^{OPE} represents a Wilson's operator expansion (OPE) of the current–current correlator in terms of quark and gluon degrees of freedom in the space-like region. On the other hand, $R^{\mathrm{HAD}}(s)$ in (19) is the same object for time-like momenta, represented by a parametrization in terms of hadronic variables. Experimentally, it can be determined by hadron production in e^+e^- reactions [28]. It is usually written in a form that exhibits the asymptotic, high momentum behavior of QCD in a manifest form:

$$\mathrm{Im}R^{\mathrm{HAD}}(s) = \Theta(s_0 - s)\,\mathrm{Im}R^{\mathrm{RES}}(s) + \Theta(s - s_0)\,\frac{1}{8\pi}\left(1 + \frac{\alpha_s}{\pi}\right), \qquad (20)$$

where s_0 denotes the threshold between the low-energy region described by a spectral function for the lowest lying resonance, $\mathrm{Im}R^{\mathrm{RES}}$, and the high-energy region described by a continuum calculated from perturbative QCD. The second term on the RHS of (20) represents the QCD perturbative result that survives when $s \to \infty$.

The dispersion integral in (19) connects time- and space-like momenta. Equation (19) also connects the hadronic (RHS) with the quark (LHS) world. It allows – after the technical step of a Borel transformation – to determine parameters in a hadronic parametrization of $R^{\mathrm{HAD}}(s)$ by comparing the LHS of this equation with its RHS.

The operator product expansion of R^{OPE} on the LHS involves a separation of momentum scales between the hard scale Q^2 and the soft, non-perturbative quark and gluon condensates [10,11]. Using the measured, known vacuum spectral function for R^{HAD} allows one to obtain information about the condensates appearing on the LHS of (19).

Turning this argument around, one can model the density dependence of the quark condensates on the LHS of (19) by using, for example, the density dependence obtained in the NJL model. The QCDSR then gives information on the density dependence of the hadronic spectral function R^{HAD} on the RHS of (19).

Since the spectral function appears under an integral the information obtained is, however, not very specific. However, Leupold *et al* [10,11] have shown that the QCDSR provides important constraints for the hadronic spectral functions in medium, but it does not fix them. Recently, Zschocke *et al* [29] have turned this argument around by pointing out that measuring an in-medium spectral function of the ω-meson could help to determine the density dependence of the chiral condensate.

Thus models are needed for the hadronic interactions. The quantitatively reliable ones can at present be based only on 'classical' hadrons and their interactions. Indeed, in lowest order in the density the mass and width of an interacting hadron in nuclear matter at zero temperature and vector density ρ_{v} are given by (for a meson, for example)

$$\begin{aligned} m^{*2} &= m^2 - 4\pi \Re f_{mN}(q_0, \theta = 0)\,\rho_{\mathrm{v}} \\ m^*\Gamma^* &= m\Gamma^0 - 4\pi \Im f_{mN}(q_0, \theta = 0)\,\rho_{\mathrm{v}}. \end{aligned} \qquad (21)$$

Here $f_{mN}(q_0, \theta = 0)$ is the forward scattering amplitude for a meson with energy q_0 on a nucleon. The width Γ^0 denotes the free decay width of the particle. For the imaginary part this is nothing other than the classical relation $\Gamma^* - \Gamma^0 = v\sigma\rho_{\mathrm{v}}$ for the collision width, where σ is the total cross-section. This can easily be seen by using the optical theorem.

Actually evaluating mass and width from (21) requires knowledge of the scattering amplitude which can only be obtained from very detailed analyses of experiments. The s-channel contributions to this scattering amplitude are determined by the properties of nucleon resonances and these are often not very well-known yet. Here, resonance physics meets in-medium physics.

Unfortunately it is not *a priori* known up to which densities the low-density expansion (21) is useful. Post *et al* [12] have recently investigated this question in a coupled-channel calculation of self-energies. Their analysis comprises pions, η-mesons and ρ-mesons as well as all baryon resonances with a sizeable coupling to any of these mesons. The authors of [12] find that already for densities less than $0.5\rho_0$ the linear scaling of the self-energies inherent in (21) is badly violated for the ρ- and the π-mesons, whereas it is a reasonable approximation for the η-meson. Reasons for this deviation from linearity are Fermi motion, Pauli blocking, self-consistency and short-range correlations. For different mesons different sources of discrepancy prevail: for the ρ- and η-mesons the iterations act against the low-density theorem by inducing a strong broadening for the $D_{13}(1520)$ and a slightly repulsive mass-shift for the $S_{11}(1535)$ nucleon resonances to which the ρ- and the η-meson, respectively, couple. The investigation of in-medium properties of mesons, for example, thus involves at the same time the study of in-medium properties of nucleon resonances and is thus a coupled-channel problem.

Note that such a picture, in which the self-energies of hadrons are generated by interactions with the surrounding baryons, also encompasses the change of the chiral condensate in (9), obtained there for non-interacting hadrons. If the spectral function of a non-interacting hadron changes as a function of density, then in a classical hadronic theory, which works with fixed (free) hadron masses, this change will show up as an energy-dependent interaction and is thus contained in any empirical phenomenological cross-section.

2.3 *Coupled channel treatment of incoherent particle production*

Very high nuclear densities (2–$8\rho_0$) and temperatures T up to or even higher than $\approx$170 MeV can be reached with present day's accelerators in heavy-ion collisions. Thus, any density-dependent effect gets magnified in such collisions. However, the observed signal always represents a time integral over quite different stages of the collision – non-equilibrium and equilibrium, the latter at various densities and temperatures. The observables thus have to be modelled in a dynamic theory. In contrast, the theoretical input is always calculated under the simplifying assumption of a hadron in stationary nuclear matter in equilibrium and at fixed density. The results of such calculations are then used in dynamical simulations of various degrees of sophistication most of which invoke a quasi-stationary approximation. In order to avoid these intrinsic difficulties we have looked for possible effects in reactions that proceed closer to equilibrium, i.e. reactions of elementary probes such as protons, pions, and photons on nuclei. The densities probed in such reactions are always $\leq\rho_0$, with most of the nucleons actually being at about $0.5\rho_0$. On the other hand, the target is stationary and the reaction proceeds much closer to (cold) equilibrium than in a relativistic heavy-ion collision. If any observable effects of in-medium changes of hadronic properties survive, even though the densities probed are always $\leq\rho_0$, then the study of hadronic in-medium properties in reactions with elementary probes on nuclei provides an essential baseline for in-medium effects in hot nuclear matter probed in ultra-relativistic heavy-ion collisions.

With the aim of exploring this possibility we have over the last few years undertaken a number of calculations for proton- [30], pion- [31,32] and photon- [33] induced reactions. All of them have one feature in common: they treat the final state incoherently in a coupled channel transport calculation that allows for elastic and inelastic scattering of, particle production by and absorption of the produced hadrons. A new feature of these calculations is that hadrons with their correct spectral functions can actually be produced and transported consistently. This is quite an advantage over earlier treatments [34,35] in which the mesons were always produced and transported with their pole mass and their spectral function was later on folded in only for their decay. The method is summarized in the following section, and more details can be found in [33].

We separate the photonuclear reaction into three steps. First, we determine the amount of shadowing for the incoming photon; this obviously depends on its momentum transfer Q^2. Second, the primary particle is produced and third, the produced particles are propagated through the nuclear medium until they leave the nucleus.

(a) *Shadowing.* Photonuclear reactions show shadowing in the entrance channel, for real photons from an energy of about 1 GeV on upwards [36]. This shadowing is due to a coherent superposition of bare photon and vector meson components in the incoming photon and is handled here by means of a Glauber multiple scattering model [26]. In this way we obtain for each value of virtuality Q^2 and energy ν of the photon a spatial distribution for the probability that the incoming photon reaches a given point; for details, see [26,37,38].

(b) *Initial production.* The initial particle production is handled differently depending on the invariant mass $W = \sqrt{s}$ of the excited state of the nucleon. If $W < 2$ GeV, we invoke a nucleon resonance model that has been adjusted to nuclear data on resonance-driven particle production [33]. If $W > 2$ GeV the particle yield is calculated with standard codes developed for high-energy nuclear reactions, i.e. FRITIOF or PYTHIA; details are given in [39]. We have made efforts to ensure a smooth transition of cross-sections in the transition from resonance physics to DIS.

(c) *Final state interactions.* The final state is described by a semiclassical coupled channel transport model that had originally been developed for the description of heavy-ion collisions and has since then been applied to various elementary reactions on nuclei with protons, pions and photons in the entrance channel.

In this method the spectral phase-space distributions of all particles involved are propagated in time, from the initial first contact of the photon with the nucleus all the way to the final hadrons leaving the nuclear volume on their way to the detector. The spectral phase-space distributions $F_h(\vec{x}, \vec{p}, \mu, t)$ give at each moment of time and for each particle class h the probability to find a particle of that class with a (possibly off-shell) mass μ and momentum $\vec{p}$ at position $\vec{x}$. Its time-development is determined by the BUU equation

$$\left(\frac{\partial}{\partial t} + \frac{\partial H_h}{\partial \vec{p}}\frac{\partial}{\partial \vec{r}} - \frac{\partial H_h}{\partial \vec{r}}\frac{\partial}{\partial \vec{p}}\right) F_h = G_h \mathcal{A}_h - L_h F_h. \tag{22}$$

Here H_h gives the energy of the hadron h that is being transported; it contains the mass, the self-energy (mean field) of the particle and a term that drives an off-shell particle back to its mass shell. The terms on the LHS of (22) are the so-called *drift terms* since they describe the independent transport of each hadron class h. The terms on the RHS of (22) are the *collision terms*; they describe both elastic and inelastic collisions between the hadrons. Here the term *inelastic collisions* includes those collisions that either lead to particle production or particle absorption. The former process is described by the *gain term* $G_h\mathcal{A}_h$ on the RHS in (22), the latter (absorption) by the *loss term* L_hF_h. Note that the gain term is proportional to the spectral function $\mathcal{A}$ of the particle being produced, thus allowing for production of off-shell particles. On the contrary, the loss term is proportional to the spectral phase-space distribution itself: the more particles there are the more can be absorbed. The terms G_h and L_h on the RHS give the actual strength of the gain and loss terms, respectively. They have the form of Born-approximation collision integrals and take the Pauli principle into account. The free collision rates themselves are taken from experiment or are calculated [33].

Equation (22) contains a self-consistency problem. The collision rates embedded in G and L determine the collisional broadening of the particles involved and thus their spectral function $\mathcal{A}$. The widths of the particles, resonances or mesons, thus evolve in time away from their vacuum values. In addition, broad particles can be produced off their peak mass and then propagated. The extra 'potential' in H already mentioned ensures that all particles are being driven back to their mass-shell when they leave the nucleus. The actual method used is described in [33]. It is based on an analysis of the Kadanoff–Baym equation that has led to practical schemes for the propagation of off-shell particles [40,41]. The possibility to transport off-shell particles represents a major breakthrough in this field. For further details of the model, see refs [33,39] and references therein.

3. Particle production on nuclei – Observables

3.1 η *Production*

We first look at the prospects of using reactions with hadronic final states and discuss the photoproduction of η-mesons on nuclei as a first example. These mesons are unique in that they are sensitive to the dominating resonance $S_{11}(1535)$ so that one may hope to learn something about the properties of this resonance inside the nuclei. Experiments for this reaction were performed both by the TAPS Collaboration [42,43] and at KEK [44].

Estimates of the collisional broadening of the $S_{11}(1535)$ resonance have given a collision width of about 35 MeV at ρ_0 [45]. The more recent, and the more refined, self-consistent calculations of [12] give a very similar value for this resonance. In addition, a dispersive calculation of the real part of the self-energy for the resonance at rest gives only an insignificant shift of the resonance position. Thus any momentum dependence of the self-energy as observed in photon-nucleus data can directly be attributed to binding energy effects [46]. The results obtained in [46] indicate that the momentum dependence of the $N^*(1535)$ potential has to be very similar to that of the nucleons.

The particular advantage of our coupled-channels approach can be seen in figure 2 which shows results both for photo- and electroproduction of η's on nuclei; for the latter process, no data are available so far. The calculations give the interesting result that for photoproduction a secondary reaction channel becomes important

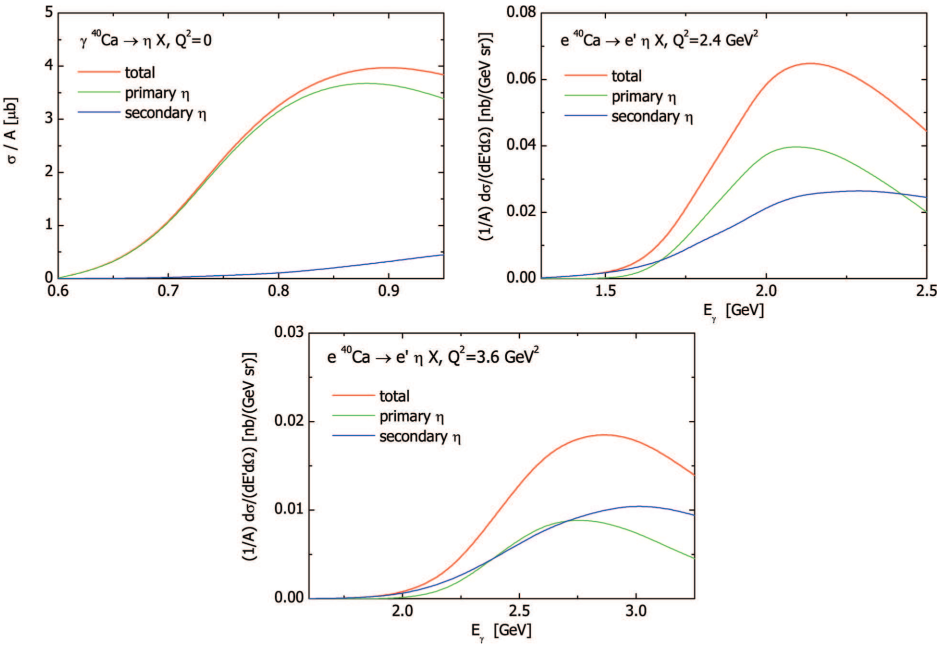

Figure 2. Eta-electroproduction cross-sections on ^{40}Ca for three values of Q^2 given in the figures. The uppermost curve in all three figures gives the total observed yield, the next curve from top gives the contribution of the direct η production channel and the lowest curve shows the contribution of the secondary process $\pi N \rightarrow \eta N$. For the highest value of $Q^2 = 3.6$ GeV^2 the primary and secondary production channels nearly coincide (from [47]).

at high energies and virtualities. In this channel first a pion is produced which travels through the nucleus and through $\pi N \rightarrow N^*(1535) \rightarrow N\eta$ produces the η that is finally observed in the experiment. This channel becomes even dominant for high Q^2 electroproduction. In both cases the reason for the growing importance of secondary production channels lies in the higher momentum transferred to the initial pion [47].

3.2 2π *production*

If chiral symmetry is restored, the masses of the scalar isoscalar σ-meson and that of the scalar isovector pion should become degenerate. This implies that the spectral function of the σ should become softer and narrower with its strength moving down to the 2π threshold. This leads to a threshold enhancement in the $\pi\pi$ invariant mass spectrum due to suppression of the phase-space for the $\sigma \rightarrow \pi\pi$ decay.

A first measurement of the two-pion invariant mass spectrum has been obtained by the CHAOS Collaboration in pion-induced reactions on nuclei [48]. The authors of [48] claimed to indeed have seen an accumulation of spectral strength near the 2π threshold for heavy target nuclei in the $\pi^+\pi^-$ mass distribution. According to the arguments presented in the introduction, photon-induced reactions in nuclei are much better suited to investigate double pion pion production at finite baryon densities. A recent experiment with the TAPS spectrometer at the tagged-photon facility MAMI-B in Mainz indeed shows an even more pronounced accumulation of spectral strength of the two-pion mass spectrum for low invariant masses with increasing target mass corresponding to increasing average densities probed [5]. This accumulation has been observed for the $\pi^0\pi^0$ but not for the $\pi^{\pm}\pi^0$ final state.

These results have been explained by a model developed by Roca *et al* [49]. In this model the σ-meson is generated dynamically as a resonance in the $\pi\pi$ scattering amplitude. By dressing the pion propagators in the medium by particle–hole loops, they found the observed downward shift of the $\pi\pi$ mass spectrum to be consistent with a dropping of the σ-pole in the $\pi\pi$ scattering amplitude, i.e. a lowering of the σ-meson mass.

In analyzing the TAPS data it is absolutely essential to simulate the final state interactions of the outgoing pions, correlated or not, in a way as realistic as possible. We have, therefore, taken the conservative approach of analyzing this reaction without any changes of the σ spectral function in the outgoing channel. The result of this study [50] is shown in figure 3.

Figure 3 shows on its left side that the observed downward shift of the $2\pi^0$ mass spectrum can be well-reproduced by final state interactions on the independent pions without any in-medium modification of the $\pi\pi$ interaction. This shift can be attributed to a slowing down of the pions due to quasi-elastic collisions with the nucleons in the surrounding nuclear medium. Also shown is the result of the

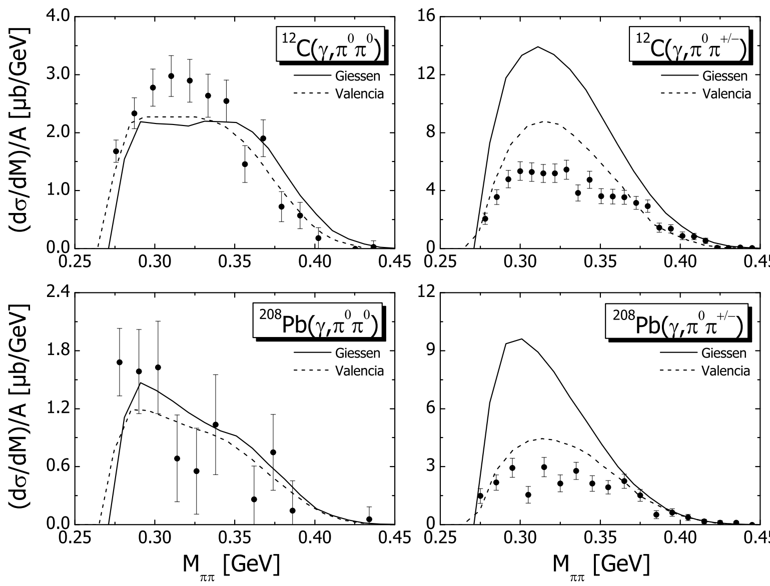

Figure 3. Two-pion invariant mass distributions for the $\pi^0\pi^0$ (left) and $\pi^0\pi^{\pm}$ (right) photoproduction on ^{12}C and ^{208}Pb (from [50]). The solid lines represent our results whereas the dashed lines labelled 'Valencia' depict the results of ref. [49].

calculations of Roca *et al* [49]. Both calculations obviously agree with each other so that the final observables are fairly independent of any $\pi\pi$ correlations.

On the right side of figure 3 the results for the semi-charged $\pi^0\pi^\pm$ channel are shown. Here our theoretical result (solid line) overestimates the data by up to a factor of 3. The result obtained in ref. [49] also lies too high, but by a lesser amount; the difference between the two calculations has been explained in [50] by the neglect of charge-transfer channels in the calculations of Roca *et al* [49]. The observed discrepancy with experiment for this channel is astounding since the method used normally describes data within a much narrower error band. Thus understanding this discrepancy is absolutely essential before a shift or non-shift in the mass distribution for this channel can be ascertained. A new analysis of the data may be helpful in this regard [51].

Even before this problem has been resolved, it is clear that pion rescattering, including charge transfer, plays a major role for the 2π mass distributions. It is, therefore, absolutely mandatory that any theoretical evaluation of this reaction takes this FSI effect into account. Because the reaction is incoherent, quantum mechanical approaches to this problem are not feasible. The semiclassical transport approaches, on the other hand, suffer from intrinsic problems at very low pion energies (in the present experiment $\approx$10 MeV kinetic energy). Here, first, the *de Broglie* wavelength of the pion is large so that semiclassical approaches have to be critically examined. Second, for these low energies the low-energy real pion potential becomes important and has to be included together with the absorptive part. Careful analyses and comparisons with optical model approaches have shown [52] that both effects introduce some systematic error into the calculations that have to be taken into account in drawing any conclusions from this experiment.

3.3 ω *Production*

Many of the early studies of hadronic properties in medium concentrated on the ρ-meson [14,53], partly because of its possible significance for an interpretation of the CERES experiment. It is clear by now, however, that the dominant effect on the in-medium properties of the ρ-meson is collisional broadening that overshadows any possible mass-shifts [12] and is thus experimentally hard to observe. The emphasis is, therefore, shifted to the ω-meson. An experiment measuring the $A(\gamma, \omega \to \pi^0\gamma')X$ reaction is presently being analyzed by the TAPS/Crystal Barrel Collaborations at ELSA [54]. The varying theoretical predictions for the ω mass (640–765 MeV) [53] and width (up to 50 MeV) [31,55] in nuclear matter at rest encourage the use of such an exclusive probe to learn about the ω spectral distribution in the nuclei.

Simulations have been performed at 1.2 GeV and 2.5 GeV photon energies, which cover the accessible energies of the TAPS/Crystal Barrel experiment. After reducing the combinatorial and rescattering background by applying kinematic cuts on the outgoing particles, we have obtained rather clear observable signals for an assumed dropping of the ω mass inside the nuclei [57]. Therefore, in this case it should be possible to disentangle the collisional broadening from a dropping mass.

One of the problems in the experimental analysis is the proper subtraction of the background observed [58]; this has so far been done in a heuristic way [59].

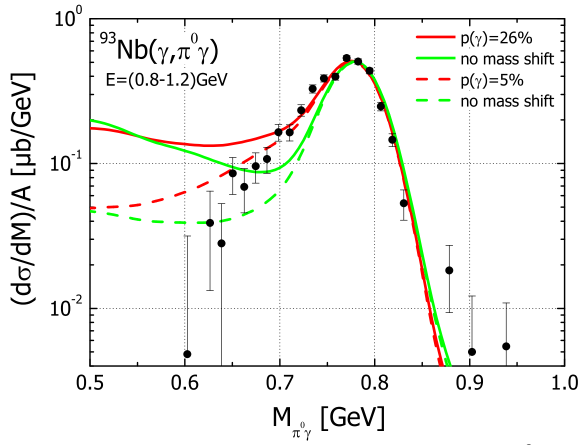

Figure 4. Mass differential cross-section for $\pi^0\gamma$ photoproduction of ^{93}Nb. Shown are the results both with and without a mass-shift as explained in [57]. The quantity p gives the escape probability for one of the four photons in the $2\pi^0$ channel. The two solid curves give results of calculations with $p = 26\%$ with and without mass-shift, the two dashed curves give the same for $p = 5\%$ (from [56]).

Our calculations represent complete event simulations. It is, therefore, possible to calculate these background contributions and to take experimental acceptance effects into account. An example is shown in figure 4 which shows the effects of a possible misidentification of the ω-meson. This misidentification can come about through the $2\pi^0 \rightarrow 4\gamma$ channel if one of the four photons escapes detection and the remaining three photons are identified as stemming from the $\pi^0\gamma \rightarrow 3\gamma$ decay channel of the ω-meson. The calculations show that the misidentification does not affect the low-mass side of the ω spectral function.

Figure 4 shows a good agreement between the data of the TAPS/CB@ELSA Collaboration [59] for a photon escape probability of 5% and a mass shift $m_\omega = m_\omega^0 - 0.18\,\rho/\rho_0$. In [57] we have also discussed the momentum-dependence of the ω self-energy in medium and have pointed out that this could be accessible through measurements which gate on different three-momenta of the ω decay products. The data presented by Trnka at this workshop [58] confirm this expectation.

3.4 *Dilepton production*

Dileptons, i.e. electron–positron pairs, in the outgoing channel are an ideal probe for in-medium properties of hadrons since they experience no strong final state interaction. The first experiment to look for these dileptons in heavy-ion reactions was the DLS experiment at the BEVALAC in Berkeley [60]. Later on, and in a higher energy regime, the CERES experiment has received a lot of attention for its observation of an excess of dileptons with invariant masses below those of the lightest vector mesons [13]. Explanations for this excess dileptons have focused on a change of in-medium properties of these vector mesons in dense nuclear matter

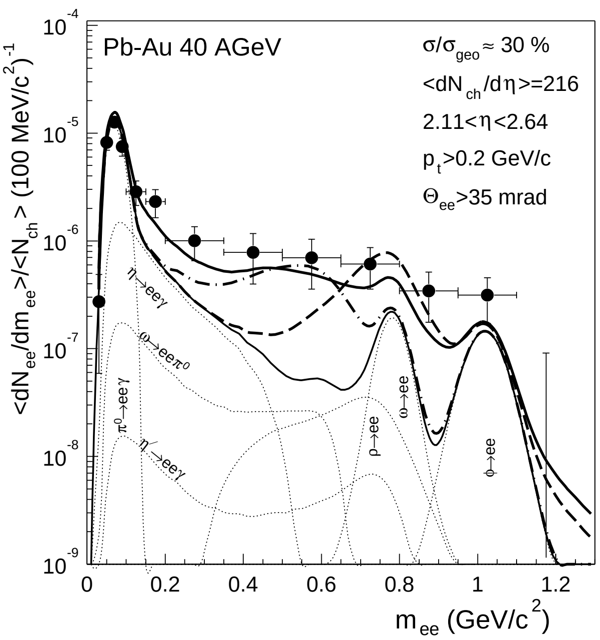

Figure 5. Invariant dilepton mass spectrum obtained with the CERES experiment in Pb + Au collisions at 40 A GeV (from [13]). The thin curves give the contributions of individual hadronic sources to the total dilepton yield, the fat solid (modified spectral function) and the dash–dotted (dropping mass only) curves give the results of calculations [19] employing an in-medium modified spectral function of the vector mesons.

(see e.g. [17,18]). The radiating sources can be clearly seen in figure 5 that shows the dilepton spectrum obtained in a low-energy run at 40 A GeV together with the elementary sources of dilepton radiation.

The figure clearly exhibits the rather strong contributions of the vector mesons – both direct and through their Dalitz decay – at invariant masses above about 500 MeV. The strong amplification of the dilepton rate at small invariant masses M caused by the photon propagator, which contributes $\sim 1/M^4$ to the cross-section, leads to a strong sensitivity to changes of the spectral function at small masses. Therefore, the excess observed in the CERES experiment can be explained by such changes as has been shown by various authors (see e.g. [34] for a review of such calculations).

In view of the uncertainties in interpreting the results discussed earlier, we have studied the dilepton photoproduction in reactions on nuclear targets. Looking for in-medium changes in such a reaction is not *a priori* hopeless: Even in relativistic heavy-ion reactions only about 1/2 of all the dileptons come from densities larger than $2\rho_0$ [34]. In these reactions the pion density gets quite large in the late stages of the collision. Correspondingly many ρ-mesons are formed (through $\pi + \pi \rightarrow \rho$) late in the collision, where the baryonic matter expands and its density becomes low again.

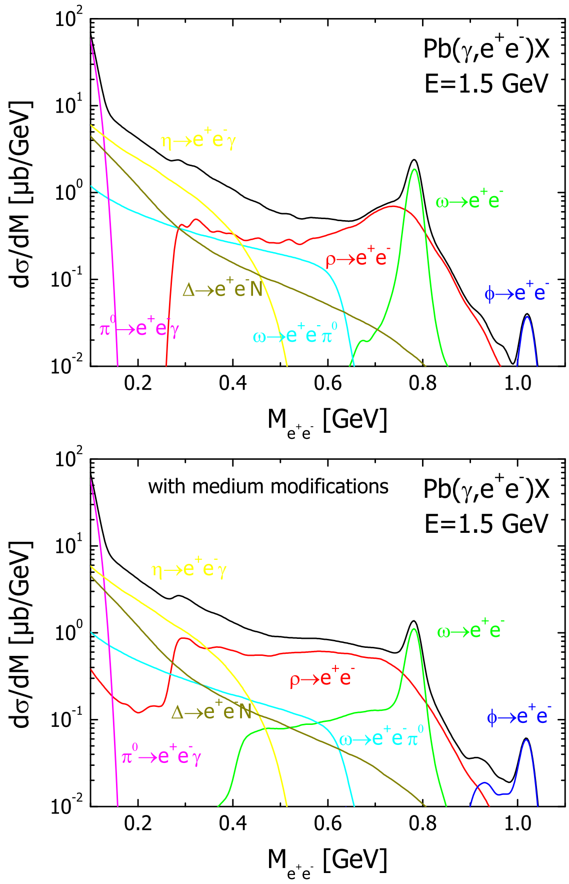

Figure 6. Hadronic contributions to dilepton invariant mass spectra for $\gamma +$ ^{208}Pb at 1.5 GeV photon energy. Indicated are the individual contributions to the total yield; compare with figure 5 (from [56]).

In [33] we have analyzed the photoproduction of dileptons on nuclei in great detail. After removing the Bethe–Heitler contribution the dilepton mass spectrum in a 2 GeV photon-induced reaction looks very similar to that obtained in an ultrarelativistic heavy-ion collision (figure 5). The radiation sources are all the same in the otherwise quite different reactions. The photon-induced reaction can thus be used as a baseline experiment that allows one to check crucial input into the simulations of more complicated heavy-ion collision.

A typical result of such a calculation for the dilepton yield – after removing the Bethe–Heitler component – is given in figure 6. The lower part of figure 6 shows that we can expect observable effect of possible in-medium changes of the vector meson spectral functions in medium on the low-mass side of the ω peak. In [33] we have shown that these effects can be drastically enhanced if proper kinematic cuts are introduced that tend to enhance the in-medium decay of the vector mesons. There it was shown that in the heavy nucleus Pb the ω peak completely disappears from the spectrum if in-medium changes of width and mass are taken into account. The sensitivity of such reactions is thus as large as that observed in ultrarelativistic heavy-ion reactions.

An experimental verification of this prediction would be a major step forward in our understanding of in-medium changes. The ongoing g7 experiment at JLAB is presently analyzing such data [61]. This experiment can also yield important information on the time-like electromagnetic form factor of the proton and its resonances [62] on which little or nothing is known.

4. Conclusions

In this lecture note I have first outlined the theoretical motivation for studies of in-medium properties of hadrons and their relation to QCD. I have then shown that photonuclear reactions on nuclei can give observable consequences of in-medium changes of hadrons that are as big as those expected in heavy-ion collisions which reach much higher energies, but proceed farther away from equilibrium. Information from photonuclear reactions is important and relevant for an understanding of high density–high temperature phenomena in ultrarelativistic heavy-ion collisions. Special emphasis was put in these lectures not so much on the theoretical calculations of hadronic in-medium properties under simplified conditions, but more on the final, observable effects of any such properties. I have discussed that for reliable predictions of observables one has to take the final state interactions with all their complications in a coupled channel calculation into account; simple Glauber-type descriptions are not sufficient.

As an example that is free from complications by FSI, I have shown that in photonuclear reactions in the 1–2 GeV range the expected sensitivity of dilepton spectra to changes of the ρ- and ω-meson properties in-medium is as large as that in ultrarelativistic heavy-ion collisions and that exactly the same sources contribute to the dilepton yield in both experiments. While the dilepton decay channel is free from hadronic final state interactions, this is not so when the signal has to be reconstructed from hadrons present in the final state. While the ω photoproduction, identified by the semi-hadronic $\pi^0\gamma$ decay channel, seems to exhibit a rather clean in-medium signal, the double-pion experiments set up to look for an in-medium shift of scalar strength in nuclei are dominated by final state interactions of the produced pions that have to be properly taken into account in any reliable analysis.

Acknowledgement

I gratefully acknowledge many stimulating discussions with L Alvarez-Ruso, O Buss, J Lehr, S Leupold, P Muehlich and M Post; many of the results discussed in these lectures are based on their work. This work has been supported by the Deutsche Forschungsgemeinschaft, partly through the SFB/Transregio 16 'Subnuclear Structure of Matter'.

References

[1] F Weber, *Prog. Part. Nucl. Phys.* **54**, 193 (2005)
[2] http://www.gsi.de/zukunftsprojekt/index.html
[3] T Ericson and W Weise, *Pions and nuclei* (Clarendon Press, Oxford, 1988)
[4] H Geissel *et al*, *Phys. Rev. Lett.* **88**, 122301 (2002)
[5] J G Messchendorp *et al*, *Phys. Rev. Lett.* **89**, 222302 (2002)
[6] A Forster *et al*, *J. Phys.* **G30**, S393 (2004)
[7] M F M Lutz and E E Kolomeitsev, *Nucl. Phys.* **A700**, 193 (2002)
[8] L Tolos, A Ramos and A Polls, *Phys. Rev.* **C65**, 054907 (2002)
[9] T Hatsuda and S H Lee, *Phys. Rev.* **C46**, 34 (1992)
[10] S Leupold, *Phys. Rev.* **C64**, 015202 (2001)
[11] S Leupold and U Mosel, *Phys. Rev.* **C58**, 2939 (1998)
S Leupold *et al*, *Nucl. Phys.* **A628**, 311 (1998)
[12] M Post, S Leupold and U Mosel, *Nucl. Phys.* **A741**, 81 (2004)
[13] J P Wessels *et al*, *Quark matter 2002 (QM 2002)*, Nantes, France, 18–24 July 2002, *Nucl. Phys.* **A715**, 262 (2003)
[14] W Peters *et al*, *Nucl. Phys.* **A632**, 109 (1998)
[15] M Post *et al*, *Nucl. Phys.* **A689**, 753 (2001)
[16] J Wambach, *Nucl. Phys.* **A715**, 422c (2003)
[17] W Cassing *et al*, *Phys. Lett.* **B363**, 35 (1995)
[18] R Rapp and J Wambach, *Adv. Nucl. Phys.* **25**, 1 (2000)
[19] R Rapp, *Pramana – J. Phys.* **60**, 675 (2003), hep-ph/0201101
[20] V Koch *et al*, *Proc. Int. Workshop XXVIII on Gross Properties of Nuclei and Nuclear Excitations*, Hirschegg, Austria, Jan. 16–22, 2000, GSI Report ISSN 0720-8715
[21] T Renk *et al*, *Phys. Rev.* **C66**, 014902 (2002)
[22] STAR Collaboration: J Adams *et al*, *Phys. Rev. Lett.* **92**, 092301 (2004)
[23] E V Shuryak and G E Brown, *Nucl. Phys.* **A717**, 322 (2003)
[24] U Mosel, *Proc. Int. Workshop XXV on Gross Properties of Nuclei and Nuclear Excitations*, Hirschegg, Austria, Jan. 13–18, 1997, p. 201, GSI Report ISSN 0720-8715
[25] U Mosel, *Proc. Int. Workshop XXVIII on Gross Properties of Nuclei and Nuclear Excitations*, Hirschegg, Austria, Jan. 16–22, 2000, GSI Report ISSN 0720-8715
[26] T Falter and U Mosel, *Phys. Rev.* **C66**, 024608 (2002)
[27] U Mosel, *Fields, symmetries, and quarks*, 2nd ed. (Springer, Heidelberg, 1999)
[28] M E Peskin and D V Schroeder, *An introduction to quantum field theory* (Addison-Wesley, Reading, 1995)
[29] S Zschocke, O P Pavlenko and B Kaempfer, *Phys. Lett.* **B562**, 57 (2003)
[30] E L Bratkovskaya, *Phys. Lett.* **B529**, 26 (2002)
[31] T Weidmann *et al*, *Phys. Rev.* **C59**, 919 (1999)
[32] M Effenberger *et al*, *Phys. Rev.* **C60**, 027601 (1999)
[33] M Effenberger, E L Bratkovskaya and U Mosel, *Phys. Rev.* **C60**, 044614 (1999)
[34] W Cassing and E L Bratkovskaya, *Phys. Rep.* **308**, 65 (1999)
[35] K Shekhter *et al*, *Phys. Rev.* **C68**, 014904 (2003)
[36] N Bianchi *et al*, *Phys. Rev.* **C60**, 064617 (1999)
[37] M Effenberger and U Mosel, *Phys. Rev.* **C62**, 014605 (2000)
[38] T Falter, K Gallmeister and U Mosel, *Phys. Rev.* **C67**, 054606 (2003); Erratum, *Phys. Rev.* **C68**, 019903 (2003)
[39] T Falter *et al*, *Phys. Rev.* **C70**, 054609 (2004)
[40] S Leupold, *Nucl. Phys.* **A672**, 475 (2000)
[41] W Cassing and S Juchem, *Nucl. Phys.* **A665**, 377 (2000)

[42] M Roebig-Landau *et al*, *Phys. Lett.* **B373**, 421 (1997)
[43] B Krusche, private communication
[44] T Yorita *et al*, *Phys. Lett.* **B476**, 226 (2000)
H Yamazaki *et al*, *Nucl. Phys.* **A670**, 202c (2000)
[45] M Effenberger *et al*, *Nucl. Phys.* **A613**, 353 (1997)
[46] J Lehr, M Post and U Mosel, *Phys. Rev.* **C68**, 044601 (2003)
[47] J Lehr and U Mosel, *Phys. Rev.* **C68**, 044603 (2003)
[48] F Bonutti, *Nucl. Phys.* **A677**, 213 (2000)
[49] L Roca, E Oset and M J Vicente Vacas, *Phys. Lett.* **B541**, 77 (2002)
[50] P Mühlich *et al*, *Phys. Lett.* **B595**, 216 (2004)
[51] S Schadmand, priv. comm.
[52] O Buss, L Alvarez-Ruso, P Muehlich and U R Shyam, nucl-th/0502031
[53] F Klingl, T Waas and W Weise, *Nucl. Phys.* **A650**, 299 (1999)
[54] J G Messchendorp *et al*, *Euro. Phys. J.* **A11**, 95 (2001)
[55] B Friman, *Acta Phys. Polon.* **B29**, 3195 (1998)
[56] P Muehlich, priv. comm.
[57] P Muehlich, T Falter and U Mosel, *Euro. Phys. J.* **A20**, 499 (2004)
[58] D Trnka, *Pramana – J. Phys.* **66**(5) (2006)
[59] CBELSA/TAPS collaboration: D Trnka, *Phys. Rev. Lett.* **94**, 192303 (2005)
[60] R J Porter *et al*, *Phys. Rev. Lett.* **79**, 1229 (1997)
[61] C Tur *et al*, JLAB experiment E-012-112
[62] U Mosel, *Proc. Int. Workshop XXIII on Gross Properties of Nuclei and Nuclear Excitations*, Hirschegg, Austria, Jan. 16–21, 1995, p. 184, GSI Report ISSN 0720-8715